JOURNAL OF CATALYSIS 58, 8–14 (1979)

The Extent of Charge Localization on Oxygen Ions and Catalytic Activity on Solid State Oxides in Allylic Oxidation of Propylene

P. A. ZHDAN, A. P. SHEPELIN, Z. G. OSIPOVA, AND V. D. SOKOLOVSKII*

Institute of Catalysis, Siberian Branch of the USSR Academy of Sciences, Novosibirsk 90, USSR

Received April 20, 1978; revised November 6, 1978

XPS and XAES methods were used to determine relative variations of the extent of charge localization on oxygen for some oxide catalysts. A relation has been found between the catalytic activity in allylic oxidation and the nucleophilic reactivity of catalyst oxygen characterized by the charge localization on oxygen ions.

I. INTRODUCTION

It is known that allylic oxidation (partial oxidation, oxidative dehydrogenation, ammoxidation) proceeds through the stage of the formation of an allylic intermediate whose rate determines the catalytic reaction rate (*1–4*). According to Ref. (*5*), the hydrocarbon activation in reactions of allylic oxidation of propylene takes place through the heterolytic dissociation of the C–H bond under the influence of a nucleophilic site—the catalyst oxygen ion. The formation of a negatively charged allylic intermediate during oxidative dehydrogenation of butene was assumed in (*6*). The relation between the catalytic activity of solid state oxides and their acid–base properties in reactions of the above type may be explained by the heterolytic character of the hydrocarbon activation (*7–9*).

According to the assumption of the heterolytic activation of allylic C–H bond during the attack by a nucleophilic site (*5*), it may be expected that the reactivity of the catalyst's oxygen at the hydrocarbon activation stage depends on the extent of the charge localization on an oxygen ion. An increase of the effective charge on an oxygen ion must facilitate the nucleophilic attack and increase the allyl oxidation rate within certain limits.

The methods of X-ray photoelectron (XPS) and X-ray Auger-electron (XAES) spectroscopy were used in the present study to compare the extent of the charge localization on oxygen ions in various catalysts. The measurements were made on the binary catalysts based on antimony oxide: tin–, gallium–, and zinc–antimony oxides known as catalysts of allyl oxidation (*4, 10, 11*) as well as on simple metal oxides involved in these systems. The reaction of propylene ammoxidation was used as an example of allyl oxidation reaction.

II. EXPERIMENTAL

1. Samples

The samples of binary catalysts Sn–Sb–O (Sn/Sb = 4); Zn–Sb–O (Zn/Sb = 0.82);

* To whom correspondence should be addressed.

0021-9517/79/070008-07$02.00/0

Ga–Sb–O (Ga/Sb = 0.43) were prepared by coprecipitation according to the procedure described in (*10*). "Pure for analysis" nitrates and chloride salts were used as reactants. The samples obtained were dried in air and calcined at 550 to 750°C for 4 hr.

2. Experimental Methods

(*a*) *X-ray photoelectron and X-ray Auger spectroscopy.* All spectra were recorded on the Vacuum Generators ESCA-3 electron spectrometer with resolution of 1.3 to 1.4 eV. The samples were treated in the preparation chamber at 200°C in oxygen (P_{O_2} = 10 Torr; 1 Torr = 133.33 N m^{-2}) for 30 to 40 min and then were transfered (without contact with atmosphere) into the analyzer chamber of the spectrometer where the spectra were recorded using the AlK_α (1486.6 eV) radiation. The spectra were recorded at a pressure of about 10^{-9} Torr at room temperature. The halfwidth of the O–$KL_{23}L_{23}$ line was 5.5 to 6.0 eV. Gold and silver were evaporated on the surface of oxides in a sample preparation chamber for corrections of the surface charge. The kinetic energy of oxygen Auger-electrons O–KLL was determined relative to the binding energies for lines $Ag3d_{5/2}$ or $Au4f_{7/2}$ ($E_{bind.}$ = 368.2 and 83.8 eV, respectively (*12*)). The accuracy of the determination of the maxima of Auger-electron lines was ±0.2 eV.

(*b*) *Catalytic experiments.* A flow installation supplied with a gradientless reactor with a vibrofluidized catalyst bed was employed to measure the rates of propylene ammoxidation. The analysis of the reaction mixture was carried out on a Hewlett–Packard chromatograph. The reaction products were passed through the trap cooled with liquid nitrogen and then through the column with molecular sieves CaA to separate (at 20°C) the reactants that were not condensed at the temperature of liquid nitrogen. The products that were condensed in the trap were heated and passed onto the column filled with Porapack-T, wherein they were separated in the mode of programmed heating (8°/min). The catalyst sample was varied from 0.1 to 1 g. The reaction mixture involved 5% C_3H_6, 6% NH_3, 18.6% O_2, 70.4% He (vol%). The reaction temperature was 450°C. The activity was determined after reaching the catalyst stationary state. The activity of the catalyst after 1 to 2 hr of operation under indicated conditions remained constant for 6 hr. The relation between the formation rate of products and the conversion degree was determined for each catalyst. The formation rates of products on catalysts were compared for similar conversions.

III. RESULTS AND DISCUSSION

(*a*) *Determination of the Character of Electron Density Variations on Oxygen in Oxides*

The electron binding energy for core and valent levels depends on the value of the effective charge on an atom (*13*). Increasing the electron density on the atom results in the decrease of BE of electrons on core levels, and vice versa, decreasing the electron density leads to the BE value increase. We may, in principle, characterize the extent of the charge localization on the atom from the core-level BE in X-ray photoelectron spectra. In particular, the charge transfer to oxygen in oxides may be determined from the energy O1S level. For example, according to Ref. (*14*), the value of E_bO1s changes regularly depending on the position of an element in the periodic system. If we move from the top to the bottom of the groups of the periodic system the binding energy of O1s level decreases with increasing the oxide basicity. If we move from the left to the right-hand side of periods this value increases. It should be noted that in some cases it is impossible to determine BE for O1s level in metal

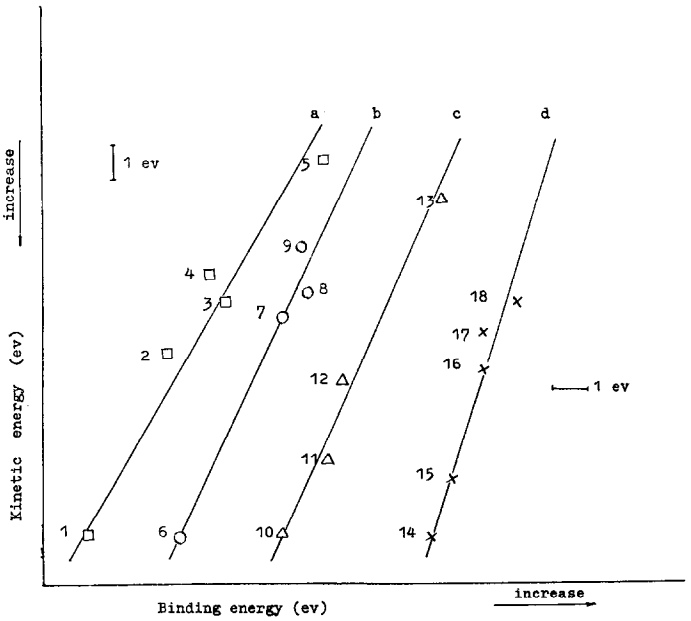

FIG. 1. Plot of Auger-electron kinetic energy versus binding energy for different compounds of As (a), Ge (b), Sb (c), Sn (d) (data taken from Ref. (*18*)); (1) As, (2) $NaAsO_2$, (3) As_2O_3, (4) Na_2HAsO_4, (5) $KAsF_6$; (6) Ge, (7) GeO_2, (8) Ge (oxidized), (9) Na_2GeF_6; (10) Sb, (11) Sb_2S_3, (12) Sb_2O_3, (13) $KSbF_6$, (14) Sn, (15) SnS, (16) Sn (oxidized), (17) Na_2SnO_3, (18) $NaSnF_5$.

oxides as the result of the imposition of the lines of the metal electron levels. For example, in antimony oxides studied the O1s line is overlapped by an intensive line of the antimony 3*d* level. Therefore, O–KLL Auger-electron spectra were used to determine the extent of the electron density localization on oxygen atoms in catalysts involving antimony.

Primary electron beams with the kinetic energy of electrons sufficient to ionize a given level are often used for obtaining Auger-spectra from solids. However, this method of excitation cannot be used for oxides since the influence of a high-energy primary electron beam results either in their reduction or decomposition. A fast dissociation was observed even in the case of a very stable oxide, such as SiO_2 (*15*). Therefore, in the present study a very soft method of excitation, i.e., X-ray radiation AlK_α with the energy of primary photons 1486.6 eV was used. Since the electron BE for 1*s* level of oxygen atom is over the range 528–533 eV (*14*), the given energy of primary X rays is quite sufficient for the ionization of electrons at the 1*s* level of oxygen and for the formation of vacancies necessary for the subsequent Auger process. The O1s lines were recorded simultaneously with Auger lines for Ga_2O_3, ZnO, and SnO_2 where no metal lines were observed in the oxygen region. The comparison of the obtained values for the photo and Auger lines enabled us to determine the character of variations of the kinetic energy for Auger electrons when BE of the 1*s* level was varied as a function of the composition.

An Auger process involves initial single ionization of a core level W and a final state x with holes in the Y and Z core levels. The kinetic energy of the Auger electron produced can be written as $E(WYZ; x)$ and, according to Shirley (*16, 17*), is related to the one-electron binding energies $E(W)$ by the equation

$$E(WYZ, x) = E(W) - E(Y) - E(Z) - F(YZ, x) + R(YZ), \quad (1)$$

where $F(YZ, x)$ is the interaction energy between the Y and Z holes in the final state and $R(YZ)$ is the total relaxation energy. If, following (*17*), we assume that the interaction energy $F(YZ, x)$ does not change with environment, the value of the shift in Auger energy can be determined as

$$\Delta E(WYZ, x) = \Delta E(W) - \Delta E(Y) - \Delta E(Z) + \Delta R(YZ). \quad (2)$$

For core levels it has been established by XPS with a good accuracy that

$$\Delta E(W) = \Delta E(Y) = \Delta E(Z), \quad (3)$$

and finally we arrive at

$$\Delta E(WYZ, x) = -\Delta E(Z) + \Delta R(YZ). \quad (4)$$

Thus, the change in the kinetic energy for Auger electrons may be opposite in sign to the shift of the core levels. Since at present theoretical estimation of $\Delta R(YZ)$ is a difficult task, we made use of the experimental data (see tables in Refs. (*18*, *19*)) on the determination of positions of the sharpest Auger—and most intense photoelectron lines for a number of compounds.

By plotting the kinetic energy of Auger electrons relative to the binding energies determined by XPS for different compounds of Sb, Sn, Ge, As (Fig. 1), it can be shown that the tendency proposed by Eq. (4) is valid, i.e., an increase in the BE of the core levels is accompanied by a decrease in kinetic energies for the corresponding Auger electrons. Estimation of the ratio $\Delta E(WYZ, x)/\Delta E(Z)$ shows that its value is more than 1, and is lying, for these compounds, in the 1.6 to 2.5 range. Differences in the proportionality coefficients may be due to the effect of polarization. This effect should be most distinct for ions with large radii, that has been actually observed in experiments (*18*).

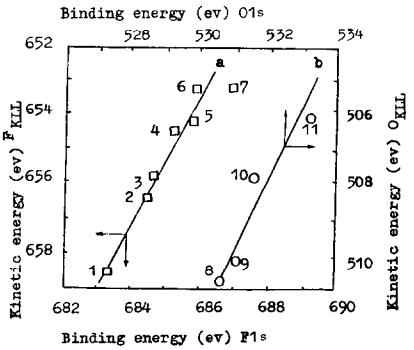

FIG. 2. Kinetic energy of KLL Auger electrons versus 1*s* binding energy for F compounds (a, data from Ref. (*19*)) and for a number of oxides (b, data of this study); (1) PbF_2, (2) CuF_2, (3) ZnF_2, (4) MgF_2, (5) Na_2GeF_6, (6) Na_2SiF_6, (7) $KSbF_6$, (8) ZnO, (9) Ga_2O_3, (10) Al_2O_3, (11) SiO_2.

TABLE 1

Energy of Oxygen Auger-Electrons $KL_{23}L_{23}$ for Simple Metal Oxides and Binary Systems

Compounds	$E_{kin}KL_{23}L_{23}$, eV
Sb_6O_{13}	509.7
Ga_2O_3	510.3
ZnO	510.7
SnO_2	510.9
Ga–Sb–O	511.2
Zn–Sb–O	511.6
Sn–Sb–O	511.9

The dependence of the O–KLL Auger line position from O1s binding energy determined in this study is given in Fig. 2 (curve b). For comparison, the experimental data for another anion, F, taken from (*19*) are also shown. These data prove the validity of Eq. (4) and point to the linear dependence of O–KLL from O1s level position. These facts provide a reliable basis for the use of O–KLL Auger line positions to determine the charge on an oxygen atom.

The values of Auger-electron energies of the $O–KL_{23}L_{23}$ transition for tin, zinc, and gallium oxides as well as for binary compounds of these oxides with antimony oxide are listed in Table 1. The data obtained indicate that the most acidic oxide Sb_6O_{13} is characterized by the lowest value of the kinetic energy of Auger electrons

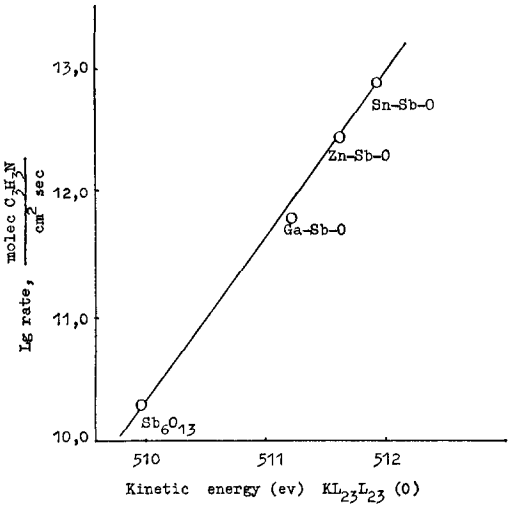

FIG. 3. The rate of acrylonitrile formation as a function of the kinetic energy of Auger electrons of oxygen on oxide antimony-containing catalysts.

as compared to more basic oxides. It should be noted that the kinetic energy value of Auger electrons for the binary system is higher than for its components. We may, therefore, propose that the basicity of the binary system is higher than that of the most basic oxide in the given pair. In a series of binary systems the energy of Auger electrons changes simultaneously with the energy variations for simple oxides of the second element, i.e., the higher basicity of the second oxide leads to the higher basicity of the binary system.

In conclusion it should be noted that the kinetic energy of the maximum of the oxygen Auger-line gives an averaged characteristic of the contacting oxygen in the system. The observed Auger-line is formed as the result of the addition of lines of various oxygen forms. For example, in complex oxides this line must involve both the component from a more nucleophilic oxygen, determined by introduction of a more basic oxide, and also a more electrophilic one bonded with antimony. Available experimental methods do not permit separation of these components. We may propose, however, that if the component of a more electrophilic oxygen is separated from the total peak in complex oxides, the maximum will be shifted toward higher energies.

Comparison of the BE values for cations in individual oxides and in binary systems in study has shown a systematic increase in BE (to 0.3–0.5 eV) for cations involved in binary systems rather than for individual oxides. It means that the more

TABLE 2

Propylene Ammoxidation on Oxide Antimony-Containing Catalysts[a]

Catalyst	Weight (g)	Surface area (m^2/g)	Contact time (sec)	Conversion (%)	Selectivity, %					
					C_3H_3N	C_3H_4O	C_2H_3N	HCN	CO	CO_2
Sb_6O_{13}	0.7	132	2.5	11.1	49.6	—	7.7	—	12.6	30.5
			4.7	16.3	42.9	—	8.8	—	11.4	32.3
			10.0	30.2	39.8	—	6.6	—	8.9	44.8
Ga–Sb–O	1.2	83	3.0	19.2	80.0	0.8	1.9	5.6	1.5	10.2
			3.3	25.0	76.0	0.9	0.8	7.0	9.5	5.9
			11.0	52.3	78.0	0.4	1.0	1.5	4.0	14.6
Zn–Sb–O	1.27	15.7	0.8	37.5	64.0	3.7	—	8.1	5.6	19.0
			2.0	48.8	62.0	1.8	1.0	14.0	4.9	16.6
			2.7	63.2	55.5	1.6	1.1	14.7	4.3	22.7
Sn–Sb–O	0.51	38	0.5	64.5	69.4	2.7	0.7	12.8	4.3	10.1
			1.2	71.8	68.5	1.6	1.4	11.6	5.1	11.8
			1.5	80.6	64.2	1.6	1.0	10.5	6.6	15.8

[a] T = 450°C, 5% C_3H_6, 6% NH_3, 18.6% O_2, 70.4% He.

negative oxygen is, the more positive are the cations. A shift to higher binding energies for the cation can prove that the charge transfer in the initial state overrides an increase in the relaxation energy during photoionization.

(*b*) *Propylene Ammoxidation*

The reaction products of ammoxidation on antimony oxide and all binary oxides were acrylonitrile, acetonitrile, hydrocyanic acid, carbon monoxide and dioxide, and small amounts of acrolein. The experimental results at different contact time are listed in Table 2. Table 3 gives the rates of acrylonitrile formation on the catalysts in study at 0 and 10% conversions. The rates obtained at 0% conversion were further used to compare them with the results of measurements of Auger-electron kinetic energy on these oxides.

TABLE 3

Acrylonitirle Formation Rates Calculated from the Data of Table 2

Catalysts	Rate, $\frac{\text{mols}}{\text{cm}^2\text{sec}} \times 10^{-11}$	
	Conversion, %	
	0	10
Sb_6O_{13}	0.20	0.16
Ga–Sb–O	6.3	5.3
Zn–Sb–O	29.0	25.0
Sn–Sb–O	32.0	74.0

IV. DISCUSSION

As we have already mentioned, according to (*5*) it may be proposed that olefin activation at the rate determining step of allylic oxidation takes place through the nucleophilic attack of the catalyst's oxygen on the allyl C–H bond. The rate of this process should depend on the nucleophility of the attacking species. The influence of the nucleophilicity of the attacking species on the reaction rate may be explained by the relation of the Swain–Scott equation type (*20*)

$$\log K = \log K_0 + \alpha N, \qquad (5)$$

where N is the parameter characterizing the nucleophility of the attacking species; α is the sensitivity of the reaction to the variation of the reactant's nucleophility; K and K_0 are the rate constants for the investigated and standard nucleophiles.

The energy of the maximum of the oxygen Auger-electron line was taken as a measure of the nucleophility in the present study. The comparison of the rates of allylic oxidation (acrylonitrile formation) with the Auger-electron kinetic energies is plotted in Fig. 3 in $\log W = f(E_{kin})$ coordinates. As seen from Fig. 3, satisfactory agreement with Eq. 5 is observed

$$\log W = A + \alpha E_{kin},$$

where $\alpha = 1.3$; $A = 9.8$ in units chosen.

The data obtained indicate that in the course of allylic oxidation the reactivity of the surface reacting oxygen may be characterized by the nucleophilicity of the catalyst's oxygen. The increase in the extent of the charge localization on the oxygen ion mentioned above must correspond to the increase in the charge of the metal ion bonded with it. It may be proposed that during activation of the C–H bond by the surface of an oxide catalyst the molecule fragments upon binding with positively and negatively charged surface centers may be shown in shorthand form as

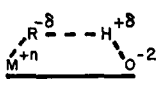

Hence, increasing the extent of the charge localization should ensure a more efficient activation due to both (i) facilitating of a nucleophilic interaction with hydrogen protonization and (ii) stabilization of an allylic fragment by the metal ion. The relative role of these factors may be

qualitatively estimated on the basis of the theory of soft and hard acids and bases (SHAB) (*21*). According to this theory, soft bases may interact efficiently with soft acids, and hard bases with hard acids. H^+ and O^{2-} represent a hard acid and base. R^- is a soft base; metal cations considered herein are either hard acids or intermediates. Owing to this, we may propose that the efficiency of the activation of the above type is primarily affected by the interaction of a nucleophilic site with hydrogen. In both cases the extent of the charge localization on oxygen ions may be used as a measure of the reactivity of the surface contact with respect to the C–H bond activation in the course of allylic oxidation.

ACKNOWLEDGMENT

The authors thank Dr. D. V. Tarasova and G. A. Zenkovets for the preparation of catalysts.

REFERENCES

1. Sachtler, W. M. H., *Rec. Trav. Chim. Pays-Bas* **82**, 243 (1963).
2. Voge, H. H., Wagner, C. D., and Stevenson, D. P., *J. Catal.* **2**, 58 (1963).
3. Adams, C. R., and Jennings, T. J., *J. Catal.* **2**, 63 (1963).
4. McCain, C. C., Gough, G., and Godin, C. W., *Nature* **198**, 58 (1963).
5. Sokolovskii, V. D., and Bulgakov, N. N., *React. Kinet. Catal. Lett.* **6**, 65 (1977).
6. Batist, Ph. A., Lippens, B. C., and Schuit, G. C. A., *J. Catal.* **5**, 55 (1966).
7. Seiyama, T., Yamazoe, N., and Egashira, M., *in* "Proceedings 5th Int. Congress Catal., 1972," Vol. 2, p. 997.
8. Tanabe, K., *Shokubay* (*Catalysts*) **17**, 72 (1975).
9. Ai, M., and Ikawa, T., *J. Catal.* **40**, 203 (1975).
10. Boreskov, G. K., Sokolovskii, V. D., Osipova, Z. G., Zenkovets, G. A., Tarasova, D. V., and Dzisko, V. A., USSR Appl. No. 530692 (1976).
11. Trifiro, F., and Sala, F., *J. Catal.* **41**, 1 (1976).
12. Johansson, G., Hedman, J., Berudtsson, A., Klasson, M., and Nilsson, R., *J. Electron. Spectrosc.* **2**, 295 (1973).
13. Siegbahn, K., Nordling, C., Fahlman, A., Nordberg, K., Hamrin, K., Hedman, J., Johansson, G., Bergmark, T., Karlsosn, S. E., Lindgren, I., and Lindberg, B., "ESCA-Atomic, Molecular, and Solid State Structure by Means of Electrons Spectroscopy." Almqvist & Wiksells, Uppsala, Sweden, 1967.
14. Nefedov, V. I., Gati, D., Dzhurinskii, B. F., Sergushin, N. P., and Salyn, Ya. V., *J. Neorg. Khim.* **20**, 2307 (1975).
15. Salmeron, M., and Baro, A. M., *Surface Sci.* **29**, 200 (1972).
16. Kowalczyk, S. P., Pollak, R. A., McFeely, F. R., Ley, L., and Shirley, D. A., *Phys. Rev.* **B8**, 2387 (1974).
17. Kowalczyk, S. P., Ley, L., McFeely, F. R., Pollak, R. A., and Shirley, D. A., *Phys. Rev.* **B9**, 381 (1974).
18. Wagner, C. D., *Faraday Disc. Chem. Soc., N* **60**, 291 (1975).
19. Wagner, C. D., *J. Electron Spectrosc. Rel. Phenom.* **10**, 305 (1977).
20. Swain, C. G., and Scott, C. B., *J. Amer. Chem. Soc.* **75**, 141 (1953).
21. Pearson, R. G., *Chem. Britain*, **3**, 103 (1967).